Available online at www.sciencedirect.com
SCIENCE DIRECT®
ELSEVIER
Polymer 47 (2006) 6004–6009
polymer
www.elsevier.com/locate/polymer

Atomistic molecular modelling of crosslinked epoxy resin

Chaofu Wu, Weijian Xu*

Institute of Polymer Research, Department of Chemistry and Chemical Engineering, Hunan University, Changsha, Hunan 410082, PR China

Received 12 March 2006; received in revised form 15 May 2006; accepted 11 June 2006
Available online 3 July 2006

Abstract

In the present study, a new method was developed to construct atomistic molecular models of crosslinked polymers based on commercially important epoxy resin. This method employed molecular dynamics/molecular mechanics schemes and assumed close proximity. The generic Dreiding2.21 force-field and advanced compass force-field were used for the construction of models and prediction of properties, respectively. A polymer network with conversion up to 93.7% was successfully generated by this method. Density and elastic constants of the system were calculated from the equilibrated structure for the validation of the generated models. The simulated results compared reasonably with experimental data available. The developed method would hold great promise in further molecular simulations for structure and properties of epoxy resin or other cured systems.

Keywords: Molecular simulation; Epoxy resin; Polymer network

1. Introduction

Epoxy resins are a big class of compounds containing two or more epoxy groups, which can react with many compounds (called curing agents) with active hydrogens such as amines and anhydrides. The resultants exhibit a series of excellent performance, i.e. high modulus and fracture strength, low creep and high-temperature performance, and thus widely serve as coatings, adhesives, composites, etc. in electronics and aerospace industries. The extensive applications continue to attract various studies on such systems [1–4]. To obtain optimized formulations and technologic conditions, numerous experiments need to be carried out. What is more, a few more experiments combined with some theories are necessary to understand some important experimental processes and phenomenon. One problem arises as to how to reduce the trials of experiments and to develop more accurate theories when confronted with the ultimate object, namely, designing molecular structures according to property requirements.

Computer simulation in turn provides an attractive complement or substitute tool. Towards developing better products, computer simulation can decrease most efforts involved in the synthesis and characterization. Thus energy requirements, environmental and economic impacts would be largely avoided or dramatically reduced. Computer simulation has been widely used to study chain structures and glass transition of polymers [5]. Two popular arithmetics are Monte Carlo simulation based the bond-fluctuation model [6–8] and molecular dynamics simulation based the bead-spring model [9–12]. These studies have been on coarse-grained models, ignoring the detailed chemical structures, and therefore cannot study the effect of structure of a specific molecule or material on properties.

On the other hand, an atomistic level simulation shows a bright promise because it allows several practical problems to be explored in detail. The atomistic molecular simulations have gained great success in the pharmaceutical industry [13,14]. Although less successful in materials, it has the potential to simulate the properties of novel materials and has become widely accepted as a powerful technique for understanding some of the properties exhibited by materials [15,16]. Many such studies have been devoted to the synthetic

---

* Corresponding author. Tel: +86 731 8821749; fax: +86 731 8821749.
E-mail address: weijxu@hnu.cn (W. Xu).

0032-3861/$ - see front matter © 2006 Elsevier Ltd. All rights reserved.
doi:10.1016/j.polymer.2006.06.025

polymer of interest for industrial applications [17–20]. It should be noted that almost all of them are carried out on the linear homopolymers or on copolymers and only seldom on the network polymers despite the importance of crosslinked copolymers in commercial applications. It is likely due to the complexity of the molecular systems, coupled with the large computational cost.

However, with the growing development of hardware and software used in molecular modelling, the time comes to the point where we can conduct several simulations on the network polymers, i.e. crosslinked epoxy resins. Fundamentally, a representative molecular structure model needs to be built and acts as an initial input of further simulations. Some methods for constructing polymer networks have been reported [21–26]. As part of our persisting interest in the simulation of crosslinked epoxy resins, we here described an alternative methodology to build fully atomistic crosslinked network systems. A detailed procedure is put forward in Section 3, followed by Section 4 on validating the models. Finally, some conclusions are drawn based on the results.

2. Molecular models of epoxy system

The calculations were made for an amine-cured epoxy as a representative example. Copolymer of epoxy resin based on diglycidyl ether bisphenol A (DGEBA) with isophorone diamine (IPD) was chosen because it is a common industrial component and appropriate experimental data are available for comparison [27]. Their molecular structures are represented in Fig. 1. For epoxy resin component DGEBA, the degree of polymerization n was set at 1. It is well understood that three principal reactions take place in this epoxy system [28], illustrated in Fig. 2 where epoxy groups react with primary amine hydrogens to form secondary amines which can in turn react with epoxy groups. So a polymer network emerges both chemically and physically. In high temperature or in the presence of catalysts, homopolymerisation of epoxy groups would also occur. Although a realistic epoxy system consists of more than epoxy resin components and curing agent components, this work represents an initial step towards developing more comprehensive realistic models of epoxy materials including other major components.

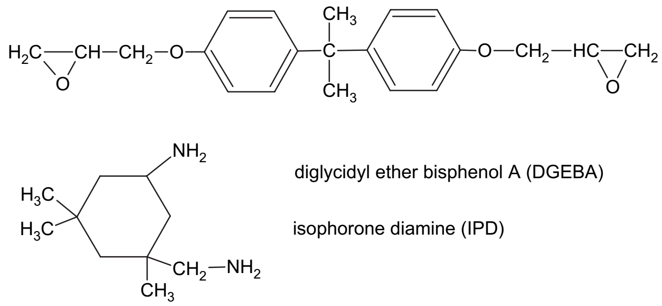

Fig. 1. Structure of resin and crosslinker molecules: top is DGEBA and bottom is IPD.

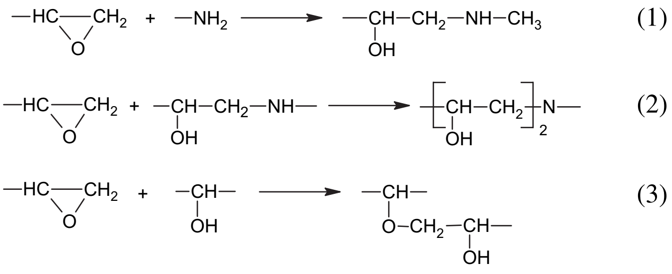

Fig. 2. Three principal reactions involved in the curing of a diamine with a diepoxide.

3. Algorithm of constructing crosslinked polymers

Polymer network was formed dynamically. To facilitate the procedure, four aspects were assumed: (1) epoxy resin component is less mobile than curing agent component; (2) primary amine hydrogen has the same reactivity to the secondary amine hydrogen; (3) the etherification reactions can be neglected; and (4) the reactions are diffusion-controlled one. According to these assumptions, the following simulation procedure was employed:

Step 1: two two-dimensional (2D) active models for small molecules DGEBA and IPD were constructed on an atom-to-atom basis. Energy minimization was performed on these two molecules to achieve reasonable three-dimensional model. Partial charges of atoms were assigned using Qeq method [29]. "Active" hydrogens on end functional groups were then removed and "reactive" molecular segments left containing reactive sites for nitrogens or carbons were used in the next step. Original, active and reactive functional groups are schemed in Fig. 3.

Step 2: 16 of reactive DGEBAs and eight of reactive IPDs were then packed into a cubic lattice corresponding to a predefined density 1.131 g cm^{-3}. The generation by means of the Amorphous Cell module in Cerius2 [30] was based on the self-avoiding random-walk method of Theodorou and Suter [31]. Periodic boundary conditions are imposed on the cubic unit cell in order to eliminate surface effects. Generated model system was employed to represent an initial physical melt mixture of the resin and crosslinker molecules with an experimental stoichiometric ratio.

Step 3: 1000 steps of energy minimization (MM) was performed followed by 1000 steps of molecular dynamics simulation (MD) to relax the central unit cell

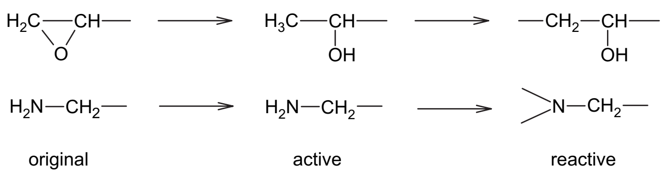

Fig. 3. Modelling of functional groups used in the construction procedure.

system. The resulting physical mixture system was analysed in order to identify the reactive sites in close proximity. One of reactive site's carbons in DGEBAs was first chosen. Then a search of nearby reactive site's nitrogens in IPDs was conducted. The reaction occurred between a pair of such reactive sites when their distance was the smallest one among possible pairs and was within a reaction cutoff distance range from 4 to 10 Å (Å $= 10^{-10}$ m).

Step 4: another circle of MM and MD was performed to relieve any unfavorable interactions due to the formation of new bonds. Then the system was checked for ring catenation or spearing possibly formed during the bond formation. When there existed any ring catenation or spearing, the new bonds would be deleted from the system. And another reactive pair with the second least distance would be scrutinized according to the same methods described above.

Step 5: the two steps (*Step 3 and Step 4*) were repeated until the conversion dropped within the range of experimental values. As the network formation nears a higher conversion, the rate of bond formation would become slowed down greatly. In order to form a more complete network in a short amount of time, the reaction radius for bond formation can be extended to a bigger value. In addition, the temperature can be raised up to a higher value to help accelerate the procedure. When the construction stops, all non-hydrogen atoms in the cell system are saturated with hydrogen atoms.

All these five steps were made as a TCL (Tool Command Language) macro program and run in the commercial molecular simulation codes Cerius2 [30] from Accelrys. The TCL was a class of script programming language originally developed by Ousterhout [32] and was designed to enhance the function of Cerius2. In terms of force-field based simulation, i.e., MM and MD, Dreiding2.21 [33] and compass [34] have been employed to study compounds containing elements C, N, O, H [35–38]. In this work we chose Dreiding2.21 force-field for construction due to its simplicity while compass was used to calculate properties of the polymer material. These force-fields describe intra-molecular and intermolecular interactions in the chemical system. The bond stretching energy, valence angle bending energy and the dihedral torsion energy are included in the bonding term for both force-fields but no cross-terms are used in the energy expression of Dreiding2.21. In the nonbonding terms, van der Waals interaction energy and coulombic interaction energy terms are included for both force-fields but no hydrogen bonding energy terms are explicitly included in compass. The second-generation force-field compass has been well parameterized and widely validated towards accurate prediction of many properties, which is expected to obtain more accurate results than the generic broadly applicable Dreiding2.21 force-field. For MM simulation in the stage of construction, the cell parameters were all fixed. For MD simulations, the NVT (constant number of molecules or atoms, volume and temperature) ensemble was used. The time step was set as 1 fs (10^{-15} s) throughout the whole simulation. Temperature was controlled at 600 K. Except noted specially, all other parameters for the calculations were set up as defaults in the Cerius2 package. To validate the resulting polymer network model, several cycles of 10,000 steps of molecular dynamics and 10,000 steps of energy minimization were performed on the generated model to reach equilibrium. Density and elastic constants were then obtained from the equilibrated structure and compared with empirical data from experiments. Different from previous stage (construction stage), the six cell parameters were all allowed to vary.

4. Results and discussion

During the past decade, several groups have reported methods for building atomistic polymer network. Hamerton and coworkers [21–23] built a set of models for polycyanurates using different methods from simple one to complex one. Their methods began with some arbitrary prepolymer with several repeat units. Yarovsky and Evans [24] and Heine and coworkers [25] developed more complex polymer network models for low molecular weight water soluble epoxy resins and end-linked poly(dimethylsiloxane) networks, respectively. The polymer networks were formed dynamically during molecular dynamics simulation in their methods. Doherty and coworkers [26] also used similar method to build poly(methacrylate) networks and called it polymerization molecular dynamics. Our method has similarity in spirits to these but is somewhat different. The main differences from ours lie in the fact that Heine introduced a new potential for bond-forming, Doherty placed the monomers on the lattice at equally distributed location and Yarovsky ran polymerization molecular dynamics only once for forming networks. Correspondingly, we used energy minimization or molecular mechanics to reduce the instability that arose from bond-forming, employed more 'liquid-like' methodologies to place the monomers and ran polymerization molecular dynamics more than once to obtain more complete conversion. Our method seems to show the potential of generating polymer network with high speed and much flexibility.

4.1. Characteristic of the system

According to the methodology described above, an epoxy resin polymer network system was successfully generated with high conversion of 93.7%. It is well known that a full conversion cannot be obtained experimentally because of gel transition and glass transition at later stage [28]. This conversion corresponds well to that of an experimental system. Although other system with different conversions can also be generated by changing reaction radius (within the reasonable range 4–10 Å), ten thousands of steps of dynamic simulations need to be carried out to form a new bond. So following discussions are restricted to this system with the highest conversion by several circles of building.

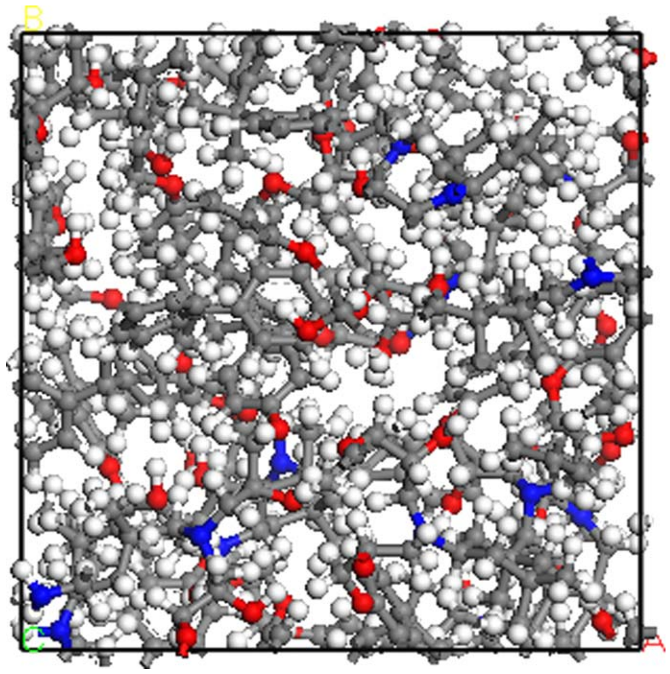

Fig. 4. Molecular model system generated according to our methods: stick-ball model, balls with different colors represent different elemental atoms (red for oxygen, gray for carbon, white for hydrogen, blue for nitrogen). (For interpretation of the references to color in this figure legend, the reader is referred to the web version of this article.)

The central unit cell of the final network system is shown in Fig. 4. As can be seen in the figure, the final network structure crosslinks together physically and chemically. Some bonds are connected to other image cells (not visualized) across the boundary and thus extend throughout the periodic cell. Due to the lack of complete experimental characterization (which can also be the reason for the sparse simulation studies on network polymer), no corresponding comparison between experiments and simulation will be specially made on the characteristic of the system. However, we can consider the crosslink effect on the molecular energy. The energy decomposition is shown in Table 1 for the cured network and for the prepolymer for comparison. It can be seen that all energy components in the cured system are higher than those in uncured ones except inversions' energy components. The differences result from newly formed bonds which confine the relaxation of the system, so the total energy rises up far from that in its natural state. However, a common characteristic is shared by the both systems: the order of contribution to total energy is same. That is, the van der Waals interaction energy and electrostatic interaction energy predominate over the others.

Table 1
Energy decomposition for the cured system and uncured system

Energy components	Cured epoxy resin system	Uncured system
Bond's stretching	234.249	166.124
Angle's bending	419.914	290.144
Torsions	280.642	201.701
Inversions	9.2901	26.24743
van der Waals	719.969	687.685
Electrostatic	−521.716	−681.710
Hydrogen bonds	−18.4308	−40.1058
Total energy	1123.92	630.086

Energy unit: kcal mol^{-1}, Dreiding2.21.

4.2. Density, volume and cell dimension of the system

To make sure the conformation of the system is stable one is necessary before calculating any static properties. This was done by considering the internal stress tensors. The components of the internal stress tensor, defined as the first derivative of the potential energy (U) per unit volume (V) with respect to strain (ε), may be calculated by summing the forces (F) acting between every pair of atoms (r for coordinates) as follows:

$$\sigma_{ij} = \frac{1}{V}\frac{\partial U}{\partial \varepsilon_{ij}} = \frac{1}{2V}\sum\left(r_i^k - r_i^l\right)F_j^{kl} \tag{1}$$

At equilibrium, the internal stress tensor must be close to 0. The root-mean-square (RMS) gradient was monitored to ensure that the minimization has properly relaxed all the degrees of freedom, calculated from the following relation:

$$\mathrm{RMS} = \sqrt{g^{\mathrm{T}}g/3N} \tag{2}$$

where g is gradient of force or stress and N the number of atoms in the system. To reach a mechanical equilibrium, energy minimization was employed again and again until a minimum in the potential energy surface (PES) was obtained. However, the obtained minimum was much sensitive to initial structure and tended to be a local minimum. So the molecular dynamics with high temperature (600 K) was carried out to pass the energy barriers to reach the "global" minimum.

The energy minimization was performed and achieved convergence to an RMS force of 0.01 kcal mol^{-1}. The internal stress components for the final system are shown in Table 2, all the values near zero indicate stress free, as anticipated for an equilibrium structure. The density obtained for this optimized system was 1.116 g cm^{-3}, a little ca. 1.5% lower than the experimental value 1.131 g cm^{-3} [27]. The error is within the general reported range. Hamerton et al. [23] obtained calculated density for bis-4-(4-cyanatophenosy)phenyl sulphone 1.20 g cm^{-3}, compared to the empirical density 1.34 g cm^{-3}. The densities of other linear polymers had 3–5% error concerning on the simulated densities [17,39,40]. When such comparison was made, some concepts needed to be remembered. The simulated densities were obtained at 0 K since molecular mechanics assumes no thermal motion of atoms while the empirical densities were measured at 298 K.

Table 2
Internal stress components of the model system

Stress components			
xx	−0.005263	*xy*	−0.02042
yy	0.001679	*yz*	0.003899
zz	−0.025909	*zx*	0.016078

Force unit: MPa, compass.

Table 3
The cell parameters for the final equilibrated system (compass)

Length	Å (10^{-10} m)	Angle	Deg (°)
a	19.81	α	80.26
b	23.60	β	92.11
c	22.04	γ	92.32

Although molecular dynamics simulation takes the temperature effect into account, much longer relaxation will be needed to be in an equilibrium. A systematic error was also regarded as the attribution to the force-field parameters [40]. In addition, a little lower conversion than the realistic one can reduce the density. Therefore, the result of density from simulation is reasonably consistent with the experimental value. For comparison, Dreiding2.21 was also used to optimize the generated structure separately. A much lower density 1.067 g cm^{-3} was obtained indicating compass was more favorable than Dreiding2.21 in the prediction of density. The cell parameters from calculation of compass are shown in Table 3. A bit bigger derivations from cubic cell indicate that the material cannot be regarded as isotropic one which can result from small size of system studied (total 1060 atoms for final system, 24 molecules or monomers for initial system). Small system was studied because of the availability of computational resource. The specific volume of the system is 10,138 Å^3 (Å $= 10^{-10}$ m).

4.3. Elastic constants (mechanical properties) of the system

Two classes of methods calculating elastic constants were available in the published articles. Consistently, static method based molecular mechanics was found more favorable than the dynamic one based molecular dynamics [41]. In this paper, a constant-strain minimization method (static method) was applied to the equilibrated system. After an initial energy minimization, a very small strain (remain within elastic limits, ±0.1%) was applied to the system and another energy minimization was started. Stiffness matrix was calculated from the second derivative of potential energy (U) with respect to strain (ε) as follows:

$$C_{ij} = \frac{1}{V}\frac{\partial^2 U}{\partial\varepsilon_i \partial\varepsilon_j} = \partial\sigma_i/\partial\varepsilon_j = (\sigma_+ - \sigma_-)/2\varepsilon_j \tag{3}$$

where σ calculated from the first derivative of potential energy per unit volume with respect to strain was stress component under tension for "+" or compression for "−". Lame constants (λ,μ) for the structure can in turn be calculated from the stiffness matrix related to

$$\begin{aligned} \lambda &= \frac{1}{3}(C_{11}+C_{22}+C_{33}) - \frac{2}{3}(C_{44}+C_{55}+C_{66}) \\ \mu &= \frac{1}{3}(C_{44}+C_{55}+C_{66}) \end{aligned} \tag{4}$$

Once the two Lame constants have been obtained, several related mechanical properties can be derived from them:

$$\begin{aligned} E &= \mu\frac{3\lambda+2\mu}{\lambda+\mu} \qquad G = \mu \\ B &= \lambda + \frac{2}{3}\mu \qquad \nu = \frac{\lambda}{2(\lambda+\mu)} \end{aligned} \tag{5}$$

where E, G, B and ν represent Young's modulus, shear modulus, bulk modulus and Poisson's ratio, respectively. An intensive description of the method can be referred to the original articles written by Theodorou and Suter [42].

For compass force-field, the entire stiffness matrix obtained from the deformed structures and undeformed structures (unit: GPa) is

$$\begin{pmatrix} 9.051 & 4.422 & 4.721 & 0.2484 & -0.5794 & -0.3849 \\ 4.384 & 8.108 & 4.446 & 0.3424 & 0.3092 & -1.208 \\ 4.701 & 4.459 & 7.949 & -0.5077 & -0.4648 & -1.324 \\ 0.2637 & 0.3663 & -0.4858 & 1.388 & 0.01599 & 0.2948 \\ -0.565 & 0.3006 & -0.0457 & 0.02091 & 2.237 & -0.03356 \\ -0.3841 & -1.236 & -2.272 & 0.2938 & -0.01258 & 2.492 \end{pmatrix} \tag{6}$$

For Dreiding2.21 force-field, the entire stiffness matrix accordingly is

$$\begin{pmatrix} 84.15 & 25.27 & 24.13 & 4.214 & 1.24685 & 3.29.40 \\ 29.87 & 74.13 & 27.84 & 8.285 & 4.400 & 2.67271 \\ 27.16 & 31.56 & 81.36 & 2.64569 & -4.922 & -7.038 \\ 1.928 & 7.506 & 2.095 & 28.88 & 0.6491 & 3.934 \\ 0.8023 & 3.519 & -5.961 & 0.4483 & 29.98 & -1.534 \\ 2.086 & 0.9828 & -7.635 & 3.711 & -1.702 & 34.07 \end{pmatrix} \tag{7}$$

Ideally, the non-diagonal components should be zero for isotropic materials. However, common characteristics of isotropic material remain in these two matrixes: the diagonal components are much higher than the non-diagonal ones and the entire matrixes are almost symmetrical along the diagonal components. The calculated elastic constants based on compass and Dreiding2.21 are represented in the Table 4 together with experimental values obtained from the literature [27]. It can be seen that the results based on Dreiding2.21 are significantly higher (about one order of magnitude) than the calculated ones based on compass and experimental values. Contrarily, the calculated results based on compass are very close to the experimental values. Once more, the compass are more favorable than the Dreiding2.21. The bulk modulus,

Table 4
Summary of data derived from the calculation for effective isotropic elastic constants

Mechanical properties	Based compass	Based Dreiding2.21	Experimental results
Bulk modulus, B (GPa)	5.804	42.92	5.01
Young's modulus, E (GPa)	5.198	47.22	4.71
Shear modulus, G (GPa)	1.924	17.93	1.75
Poisson's ratio, ν	0.3507	0.32	–

Young's modulus and shear modulus are consistently a little about 15% higher than the corresponding experimental values. This trend as upper limit has also been reported by other groups [41,43,44]. This may partly result from the fact that the models for calculation represent perfect structure while realistic systems have voids or defects in the structures. A little lower conversion compared to the experimental value may be also responsible for it. The Poisson's ratio drops in the range of general polymer materials 0.33–0.38 [44]. From these results, the compass reproduced well experimental measurements. Although more accurate values can be obtained by averaging several different structures [45], no repeats were done in this work for the purposes of validation. Good agreements between the calculated elastic constants and the experimental values confirmed that the models developed on the basis of the newly developed method are representative.

5. Conclusions

In the current study, a new method for the construction of atomistic polymer network was developed and applied to epoxy resin system based on DGEBA and IPD. The advantages when combined with powerful hardware and software are its high speed and flexibility. For example, it can generate various polymer network with different conversions by several building circles. In this work, polymer network with up to 93.7% conversion was successfully generated and studied. Compass force-field and Dreiding2.21 force-field were used separately to obtain the density and elastic constants of the system. The former compared more favorably with the corresponding experimental values than the latter. It showed the great importance of force-field in accurate prediction of structure and properties. Good agreement between the simulated properties and the experimental values considering some possible error origins indicated that the generated polymer network was representative for realistic system. It can be expected that the developed method would be employed in further molecular simulation of structure and properties for crosslinked epoxy resin or other cured polymer network.

Acknowledgements

Chaofu Wu wishes to acknowledge his wife, Wanhua Yang, and her parents who gave him continuous encouragement and supports in spirits and the center of molecular simulation (situated at Hunan University) in Hunan province which provided computational platform (SGI workstation and Cerius2 package) for completing this work.

References

[1] Liu H, Uhlherr A, Bannister MK. Polymer 2004;45:2051–60.
[2] Ni Y, Zheng S, Nie K. Polymer 2004;45:5557–68.
[3] Liu Y, Zheng S, Nie K. Polymer 2005;46:12016–25.
[4] Boinard P, Banks WM, Pethrick RA. Polymer 2005;46:2218–29.
[5] Binder K, Baschnagel J, Paul W. Prog Polym Sci 2003;28:115–72.
[6] Carmesin I, Kremer K. Macromolecules 1988;21:2819–23.
[7] Jo WH, Ko MB. Macromolecules 1993;26:5473–8.
[8] Jo WH, Ko MB. Macromolecules 1994;27:7815–24.
[9] Stevens MJ. Macromolecules 2001;34:1411–5.
[10] Stevens MJ. Macromolecules 2001;34:2710–8.
[11] Tsige M, Stevens MJ. Macromolecules 2004;37:630–7.
[12] Tsige M, Lorenz CD, Stevens MJ. Macromolecules 2004;37:8466–72.
[13] Perun TJ, Propst CL. In: Perun TJ, Propst CL, editors. Computer-aided drug design: methods and applications. New York: Marcel Dekker Inc; 1989.
[14] Charifson PS. Practical application of computer-aided drug design. New York: Marcel Dekker Inc; 1997.
[15] Madkour TM, Barakat AM. Comput Theor Polym Sci 1997;7:25–46.
[16] Kremer K. Macromol Chem Phys 2003;204:257–64.
[17] Kang JW, Choi K, Jo WH, Hsu SL. Polymer 1998;39:7079–87.
[18] Pavel D, Ball J, Bhattacharya S. J Polym Sci Part B Polym Phys 1999;37:2334–52.
[19] Liang T, Yang X, Zhang X. J Polym Sci Part B Polym Phys 2001;39:2243–51.
[20] Eichinger BE, Rigby D, Stein J. Polymer 2002;43:599–607.
[21] Hamerton I, Heald CR, Howlin BJ. J Mater Chem 1996;6:311–4.
[22] Hamerton I, Howlin BJ, Klewpatinond P, Takeda S. Polymer 2002;43:4599–604.
[23] Hamerton I, Howlin BJ, Klewpatinond P, Shortley HJ, Takeda S. Polymer 2006;47:690–8.
[24] Yarovsky I, Evans E. Polymer 2002;43:963–9.
[25] Heine DR, Grest GS, Lorenz CD, Tsige M, Stevens MJ. Macromolecules 2004;37:3857–64.
[26] Doherty DC, Holmes BN, Leung P, et al. Comput Theor Polym Sci 1998;8:169–78.
[27] Sindt O, Perez J, Gerard JF. Polymer 1996;37:2989–97.
[28] Girard-Reydet E, Riccardi CC, Sautereau H, et al. Macromolecules 1995;28:7599–607.
[29] Rappé AK, Goddard WA. J Phys Chem 1991;95:3358.
[30] Accelrys Inc, San Diego, CA, USA (OFF, Amorphous builders).
[31] Theodorou DN, Suter UW. Macromolecules 1985;18:1467–78.
[32] Ousterhout JK. Tcl and the Tk toolkit. Reading: Addison-Wesley; 1994.
[33] Mayo SL, Olafson BD, Goddard WA. J Phys Chem 1990;94:8897–909.
[34] Sun H. J Phys Chem B 1998;102:7338.
[35] Barton JM, Buist GJ, Deazle AS, Hamerton I, Howlin BJ, Jones JR. Polymer 1994;35:4326–33.
[36] Barton JM, Deazle AS, Hamerton I, Howlin BJ, Jones JR. Polymer 1997;38:4305–10.
[37] Mijovic J, Zhang H. J Phys Chem B 2003;108:2557–63.
[38] Mijovic J, Zhang H. Macromolecules 2003;36:1279–88.
[39] Fan CF, Ling HSU. Macromolecules 1991;24:6244–9.
[40] Vasudevan VJ, McGrath JE. Macromolecules 1996;29:637–45.
[41] Raaska T, Niemela JS, Sundholm F. Macromolecules 1994;27:5751–7.
[42] Theodorou DN, Suter UW. Macromolecules 1986;19:139–54.
[43] Fan CF, Hsu SL. Macromolecules 1992;25:266–70.
[44] Fan CF, Cagin T, Chen ZM. Macromolecules 1994;27:2383–91.
[45] Suter UW, Eichinger BE. Polymer 2002;43:575–82.